

LA-6188

c.3

CIC-14 REPORT COLLECTION  
**REPRODUCTION  
COPY**

UC-34c

Issued: January 1977

## $^4\text{He}(t, t)^4\text{He}$ Elastic Scattering: Analyzing Powers and Differential Cross Sections

by

R. A. Hardekopf  
Nelson Jarmie  
G. G. Ohlsen  
R. V. Poore  
R. F. Haglund, Jr.  
Ronald E. Brown\*  
P. A. Schmelzbach\*\*  
B. D. Anderson†  
D. M. Stupin  
P. A. Lovoi††



\*Visiting Staff Member. University of Minnesota, Minneapolis, MN 55455.

\*\*Long-Term Visiting Staff Member. Eidgenoessische Technische Hochschule, Zürich, Switzerland.

†Guest Scientist. Kent State University, Kent, OH 44242.

††Associated Western Universities, Inc., Graduate Student. ILC Technology, Inc., 164 Commercial Street, Sunnyvale, CA 94086.



**los alamos**  
**scientific laboratory**  
of the University of California  
LOS ALAMOS, NEW MEXICO 87545



An Affirmative Action/Equal Opportunity Employer

UNITED STATES  
ENERGY RESEARCH AND DEVELOPMENT ADMINISTRATION  
CONTRACT W-7408-ENG. 38

Printed in the United States of America. Available from  
National Technical Information Service  
U.S. Department of Commerce  
5285 Port Royal Road  
Springfield, VA 22161

Price: Printed Copy \$3.50 Microfiche \$3.00

This report was prepared as an account of work sponsored by the United States Government. Neither the United States nor the United States Energy Research and Development Administration, nor any of their employees, nor any of their contractors, subcontractors, or their employees, makes any warranty, express or implied, or assumes any legal liability or responsibility for the accuracy, completeness, or usefulness of any information, apparatus, product, or process disclosed, or represents that its use would not infringe privately owned rights.

**${}^4\text{He}(t,t){}^4\text{He}$  ELASTIC SCATTERING:  
ANALYZING POWERS AND DIFFERENTIAL CROSS SECTIONS**

by

R. A. Hardekopf, Nelson Jarmie, G. G. Ohlsen, R. V. Poore,  
R. F. Haglund, Jr., Ronald E. Brown, P. A. Schmelzbach,  
B. D. Anderson, D. M. Stupin, and P. A. Lovoi

**ABSTRACT**

Analyzing power and differential cross-section results are presented in tabular and graphical form for  ${}^4\text{He}(t,t){}^4\text{He}$  elastic scattering from 7- to 14-MeV bombarding energy. The experimental procedure is described for measuring the analyzing powers.



## I. INTRODUCTION

This report presents tabulations and graphs of  ${}^4\text{He}(t,t){}^4\text{He}$  elastic scattering data obtained recently at the Los Alamos Scientific Laboratory tandem Van de Graaff facility. The analyzing power data result from the first experiment performed with a polarized triton source;<sup>1</sup> the experimental procedure is included for this reason. Details of the differential cross-section experiment are reported elsewhere,<sup>2</sup> but the data from that experiment are included here for completeness.

## II. EXPERIMENTAL EQUIPMENT AND PROCEDURE FOR ANALYZING POWER MEASUREMENTS

The analyzing power experiment was performed with a polarized triton beam striking a  ${}^4\text{He}$  gas target. Two detectors at symmetric angles each simultaneously monitored scattered tritons and recoil alphas to collect data from which the analyzing powers were obtained.

The polarized triton beam was focused onto the target at the center of the supercube<sup>3,4</sup> scattering

chamber. The beamline plan is shown in Fig. 1. Entrance slits to the chamber ( $2.54 \text{ mm}^2$ ) were located 60.6 cm from the center of the target. A set of antiscatter slits ( $3.05 \text{ mm}^2$ ) were located 40.3 cm from the target center. A circular collimator 2.54 mm in diameter preceded the  $2.5\text{-}\mu\text{m}$ -thick target entrance foil, and antiscatter baffles followed it. After passing through the target, the beam was collected on the chamber exit slits 65.6 cm from target center as well as on the Faraday cup which followed. A beam position indicator simultaneously displayed the current intercepted by the first set of entrance slits and by the exit slits. Beam position was maintained throughout the experiment by keeping the current on these slits balanced in the left-right and up-down directions. Currents on the exit slits were added to the Faraday cup current, and the total was recorded by a current integrator.

The target, shown schematically in Fig. 2, was a 10-cm-diam cylindrical gas cell pressurized with  ${}^4\text{He}$  to 300 torr and covered at first with  $2.5\text{-}\mu\text{m}$ -thick Havar foil, then later with  $6.3\text{-}\mu\text{m}$ -thick Kapton plastic film. For measurements with the Kapton film, a 3-*l* buffer was attached to the gas-cell filler tube to compensate for diffusion losses through the film.

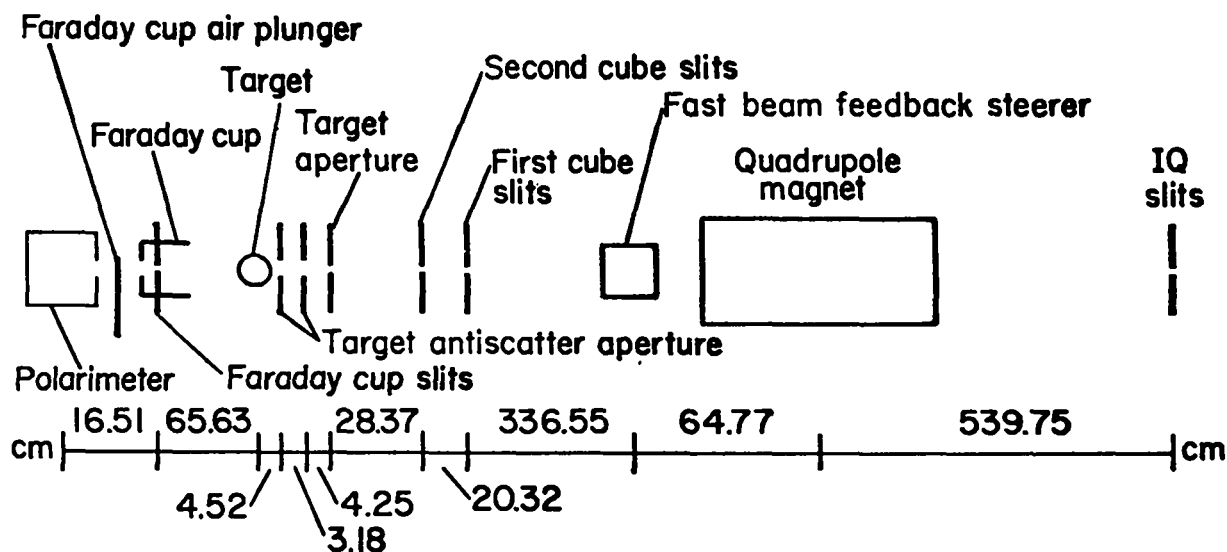


Fig. 1.

Supercube scattering chamber beamline plan (not to scale). Slit sizes are given in the text.

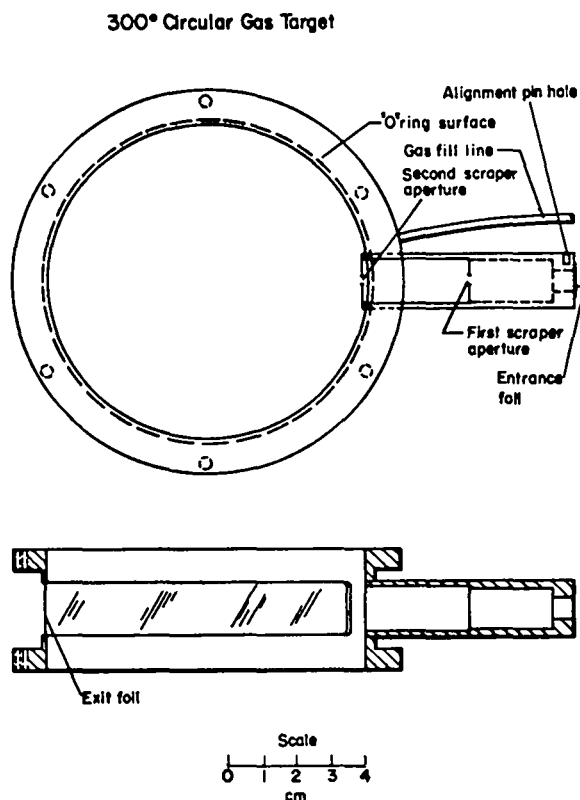


Fig. 2.

Schematic of 300° circular target. The target was pressurized to 300 torr with  $^4\text{He}$ .

Two detector telescopes viewed the target at equal angles left and right of the beam axis. Figure 3 shows the detector snouts used with the gas target. Each detector collimator consisted of a front rectangular slit 5.1 cm from the target center and a rear rectangular slit 24.1 cm from the target center. Both collimator apertures were 3.33 mm wide by 11.4 mm high, giving an angular resolution of  $1.0^\circ$ , full width at half maximum (FWHM). Mean scattering angles were determined to  $\pm 0.05^\circ$ . Further details on the collimators, antiscatter slits, and supercube hardware can be found in Ref. 4.

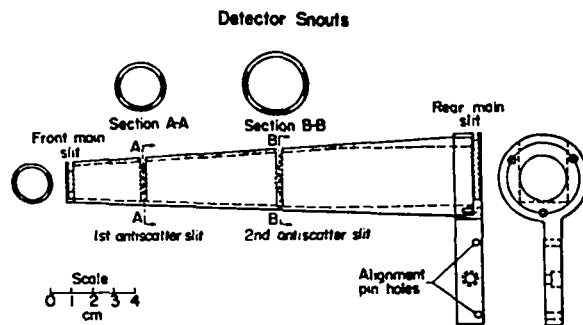


Fig. 3.

Detector snouts used to hold collimators for gas target geometry. The dimensions of the collimator slits are given in the text.

Each counter telescope contained a 48- $\mu\text{m}$ -thick-thick  $\Delta\text{E}$  detector and a 1000- $\mu\text{m}$ -thick E detector. For those events which gave rise to a  $\Delta\text{E}$ -E coincidence, linear  $\Delta\text{E}$  and E signals were sent to analog-to-digital converters (ADCs) and stored in an on-line computer. Mass identification was performed by computer processing; events resulting from tritons and recoil alpha particles were stored in separate memory blocks. Alpha particles penetrated  $\Delta\text{E}$  detectors only for higher energies and forward angles. Therefore,  $\Delta\text{E}$  singles spectra were simultaneously stored by means of separate ADCs. Most alpha particle data were obtained in this *singles* mode.

Peak sums were obtained on-line by setting relatively narrow gates on the peaks. A visually satisfactory linear background line was set by means of a wider "background gate," and the linear background under the peak was subtracted in the analysis routine. For most of the data, the background counts thus obtained were much less than 1% of the peak sums. For some of the data where alpha particles were detected in *singles* mode, background counts approached 3%. Even in these cases the analyzing power calculations, with and without background correction differed by less than statistical error. Corrected counts were used for the final tabulation.

The data acquisition sequence for each angle consisted of runs of equal integrated charge for triton beam polarization in the up-down directions. Beam polarization  $P_Q$  was determined by averaging quench-ratio<sup>8</sup> results obtained before and after each run. These results were determined from the accelerated beam by a computer routine that measures, with a digital picoammeter, the ratio Q of normal beam current to quenched beam current and calculates

$$P_Q = 1 - \frac{1}{Q}$$

Two measurements of  $P_Q$  were made each time the routine was called; their average was stored in the computer. In this manner, eight  $P_Q$  values were averaged for a spin-up, spin-down sequence. The final average  $\bar{P}_Q$  was used in calculating the analyz-

ing power. Accuracy of the quench-ratio technique for triton beam polarization was one of the results determined in this experiment: it was found to be accurate to within  $\pm 0.010$  (Ref. 6).

Analyzing powers  $A_y$  were calculated from the geometric average of left (L) and right (R) detector yields for the two runs:

$$r = \left( \frac{L\uparrow R\downarrow}{R\uparrow L\downarrow} \right)^{1/2}$$

$$A_y = \frac{1}{P_Q} \left[ \frac{r - 1}{r + 1} \right]$$

where the arrows indicate spin-up and spin-down beam polarizations. This method cancels the effects of differences in detector efficiency and of errors in current integration.<sup>7</sup> Data acquisition and processing, quench-ratio measurements, spin-direction control of the polarized source,  $A_y$  calculations, and detector angle changes in the scattering chamber were entirely under computer control. This freed the experimenter to concentrate on setting foreground and background gates in the spectra and to monitor the data acquisition.

An important correction is necessary to both the analyzing power and cross-section data when there is a combination of a large curvature in the angular distribution and a significant multiple scattering of the detected particles in the target exit foil. In this case, the particles multiply-scattered into and away from the detector did not completely compensate each other. The effect was especially serious for the sharp peaks at large c.m. angles where alpha particles were detected. With a Havar foil target, corrections as large as 14% in the cross section and 0.1 to 0.2 in the analyzing power were necessary. Much of the  $A_y$  data and some of the cross-section data, where alphas were detected, were rerun with the target gas contained by a Kapton film. Approximate correction formulas<sup>8</sup> and a Monte Carlo program<sup>9</sup> were developed and used to make corrections (usually less than 3%) to the cross-section data. The results of the runs with a Kapton target, the formulas, and the Monte Carlo program were consistent. Larger-than-normal errors seen in parts of the data are the result of the above problem.

### III. ANALYZING POWER DATA

Complete angular distributions of the analyzing powers were obtained at three energies: 8.785, 10.815, and 12.250 MeV. Partial distributions were obtained at four other energies from 10.2-11.7 MeV near the angular region where  $A_y$  approaches its minimum possible value of  $-1$ . These data have been discussed in Ref. 10. In addition to an extensive excitation function at  $\Theta_{lab} = 28.5^\circ$ , some excitation function data were obtained at  $\Theta_{lab} = 35.0^\circ$  near the energy where a Wigner Cusp effect<sup>2,11,12</sup> was expected.

Energy of the bombarding beam was known to  $\pm 15$  keV with a FWHM spread of 40 keV including the effects of foil and target-gas straggling and machine energy resolution. The relative energy of adjacent runs in an excitation function is accurate to  $\pm 5$  keV.

Analyzing power data obtained with the polarized triton beam are summarized in Tables I and II. Numerical data are tabulated in Appendix A. Figures 4-6 show the polarization data in graphical form. Shown for comparison in Fig. 5 are data from Ref. 13.

The relative accuracy of the data is generally better than  $\pm 0.020$ , and much of it is better than  $\pm 0.007$ . Relative errors listed in Appendix A are primarily statistical, although when the statistical error was less than  $\pm 0.007$ , we took this value as a lower limit. The limit results from our knowledge of the background and from our observation of maximum fluctuation in quench-ratio determinations of beam polarization. It also derives from our observations over many years of the reproducibility of proton analyzing power data taken with similar techniques. We believe the scale error for these measurements (i.e., the amount they could be renormalized in order to minimize  $\chi^2$  in a search) to be 1%. This is a multiplicative factor based on long-term observations of the quench-ratio accuracy under varying operating conditions of the polarized source.

The data at 10.200, 11.100, 11.390, and 11.700 MeV near the  $A_y = -1$  point (see Fig. 6) have not been corrected for multiple scattering (since the curvatures are obscure), nor repeated with a Kapton target. The points that might have a significant correction are in those at  $100^\circ$  c.m. and larger. This will not affect the conclusions of the analyzing power

TABLE I

#### RANGE OF ANGULAR DISTRIBUTIONS FOR $A_y(\theta)$

<u>Energy</u> (MeV)	<u><math>\Theta_{c.m.}</math></u> (deg)	<u>Data</u> <u>Points</u>
8.785	26-150	31
10.200	61-110	12
10.815	28-148	58
11.100	56-115	14
11.390	61-110	12
11.700	61-110	12
12.250	26-150	30

TABLE II

#### RANGE OF EXCITATION FUNCTIONS FOR $A_y(\theta)$

<u>Energy</u> (MeV)	<u><math>\Theta_{lab}</math></u> (deg)	<u><math>\Theta_{c.m.}</math></u> (deg)	<u>Data</u> <u>Points</u>
7.000-14.200	28.5 <sup>a</sup>	49.6	60
7.000-14.200	28.5 <sup>b</sup>	123.0	15
8.200-8.870	35.0 <sup>a</sup>	60.6	12
8.200-8.870	35.0 <sup>b</sup>	110.0	12

<sup>a</sup>Tritons.  
<sup>b</sup>Alphas.

calibration in Ref. 10, but these particular data should be used with caution in a numerical analysis.

A preliminary report of the polarization data has been presented.<sup>6,10,14</sup>

### IV. DIFFERENTIAL CROSS-SECTION DATA

The differential cross-section data<sup>2</sup> included in this report were taken with an unpolarized triton

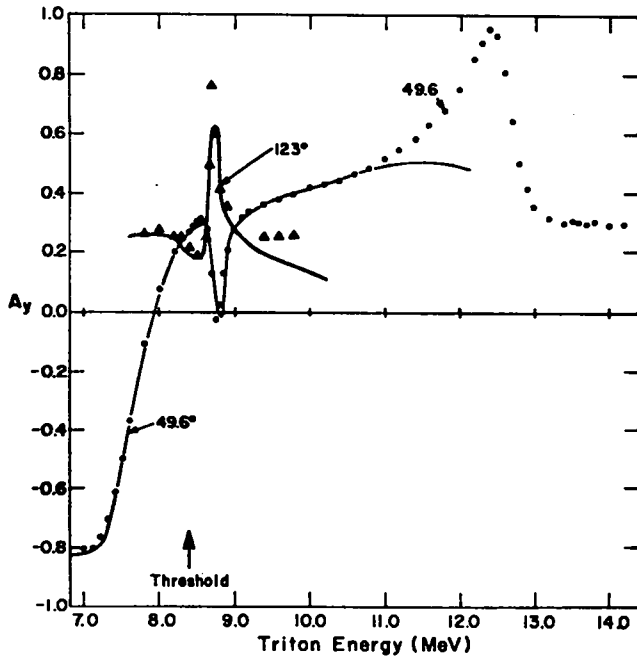


Fig. 4.  
Excitation function for the  ${}^4\text{He}(t,t){}^4\text{He}$  analyzing power.

beam in an Ortec\* 60-cm scattering chamber. Relative and scale errors are listed in the tabulations. Energy errors are the same as those discussed with the analyzing power data. Angular width of the double-slit system was  $0.3^\circ$  FWHM, and the final accuracy of the measured angle was  $\pm 0.03^\circ$ .

Tables III and IV summarize the differential cross-section data; complete tables are provided in Appendix B. Figures 7 and 8 show the data in graphical form.

## V. DISCUSSION

Experimental procedures and numerical data have been reported for accurate measurements of the  ${}^4\text{He}(t,t){}^4\text{He}$  reaction from 7 to 14 MeV. Both the analyzing power data and differential cross-section data are presently being used (with data from other laboratories in both the alpha + triton and  ${}^6\text{Li}$  + neutron channels) in an R-matrix analysis of the  ${}^7\text{Li}$  system.<sup>16</sup> The solid lines in Figs. 4, 5, 7, and 8 are preliminary R-matrix predictions which were obtained without using a complete set of the present

\*Ortec Inc., Oak Ridge, TN. 37830.

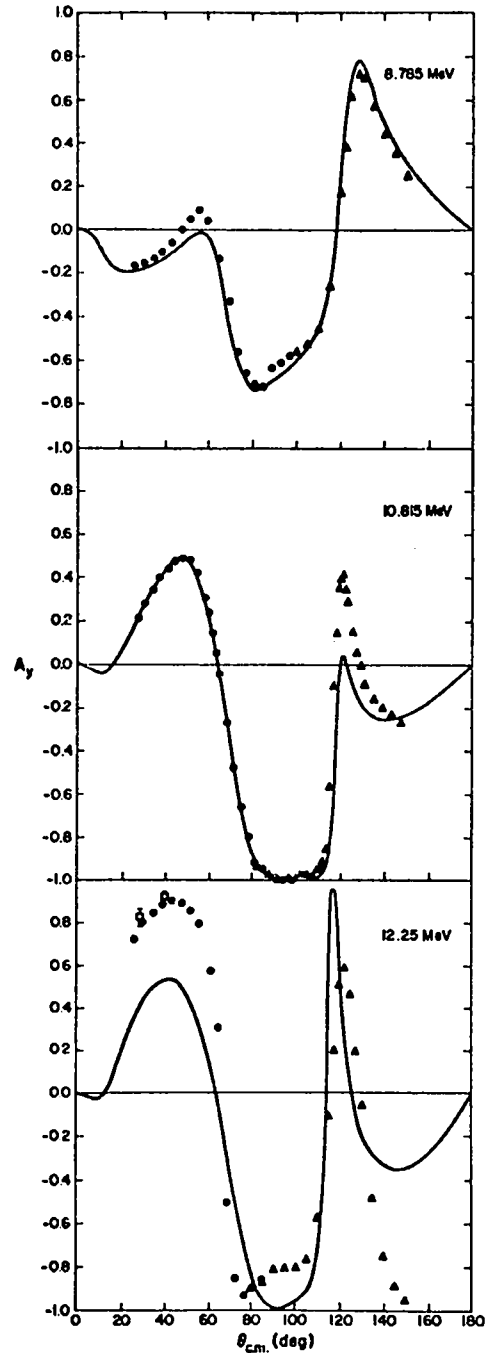


Fig. 5.  
Angular distributions of the analyzing power for  ${}^4\text{He}(t,t){}^4\text{He}$  elastic scattering. The open square points at low angles at 12.25 MeV are from the double-scattering measurements of Keaton et al. (Ref. 13).

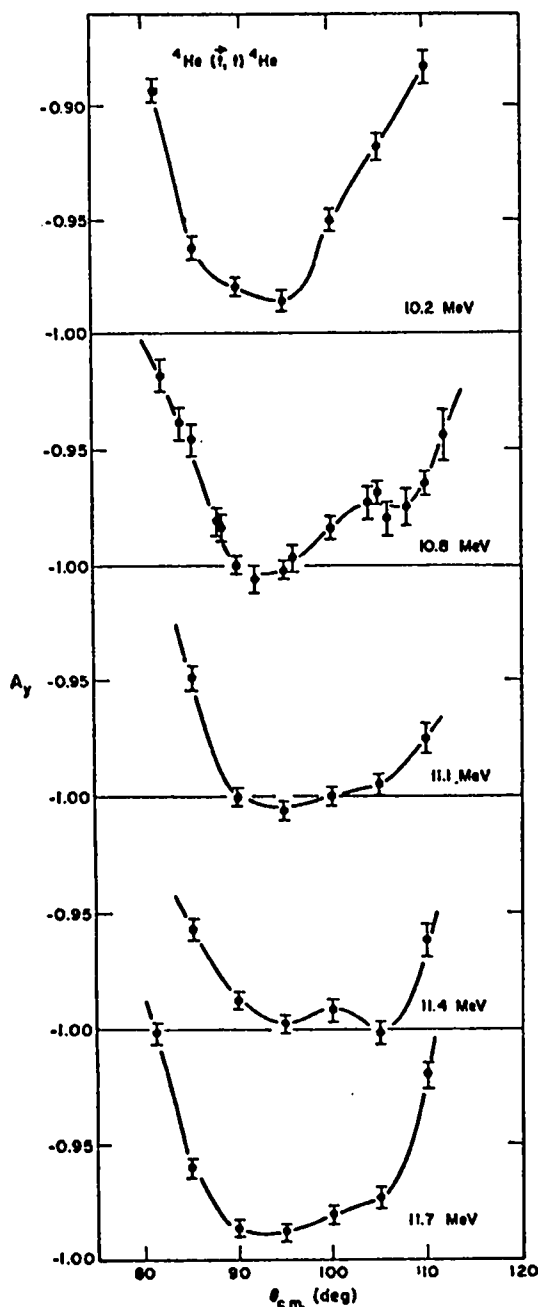


Fig. 6.

Angular distributions of the analyzing power for  ${}^4\text{He}(t,t){}^4\text{He}$  elastic scattering near  $A_y = -1$ . Solid lines only connect data points as a visual guide.

data, in particular the final analyzing powers. The indication is that both the cross sections and the analyzing powers will have a strong influence on the fit.

TABLE III  
RANGE OF ANGULAR  
DISTRIBUTIONS FOR  $\sigma(\theta)$

Energy (MeV)	$\theta_{\text{c.m.}}$ (deg)	Data Points
8.230	22-155	22
8.580	22-155	18
8.790	22-155	17
8.980	22-155	24
9.880	22-155	27
12.000	22-155	17

TABLE IV  
RANGE OF EXCITATION FUNCTIONS  
FOR  $\sigma(\theta)$

(Energy = 7.600-10.000 MeV)

$\theta_{\text{lab}}$ (deg)	$\theta_{\text{c.m.}}$ (deg)	Data Points
15.0 <sup>a</sup>	26.3	21
15.0 <sup>b</sup>	150.0	21
28.5 <sup>a</sup>	49.6	22
28.5 <sup>b</sup>	123.0	21
40.0 <sup>a</sup>	69.0	21

<sup>a</sup>Tritons.  
<sup>b</sup>Alphas.

Although it is not apparent in the figures as drawn, a careful study of the data and the R-matrix fit does indicate a slight anomaly near 8.4 MeV where a Wigner Cusp<sup>11,12</sup> is expected. The effect is certainly not very marked, and further precision experiments should be done if the nature of the cusp is to be explored.



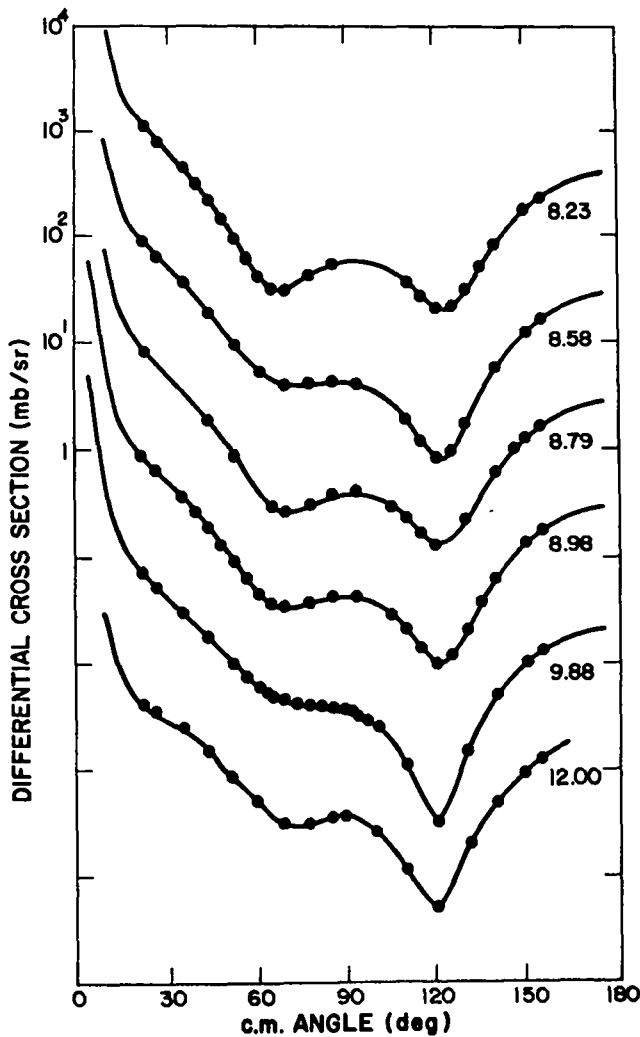


Fig. 7.  
Angular distributions of the differential cross section for  ${}^4\text{He}(t,t){}^4\text{He}$  elastic scattering.

#### ACKNOWLEDGMENTS

It is a pleasure to acknowledge the assistance of Louis Morrison in the construction of the polarized triton source and the experimental apparatus. We are also indebted to D. C. Dodder and G. M. Hale for providing the predictions of their R-matrix analysis before publication. H. C. Britt, J. Sunier, and R. J. Barrett helped greatly taking data in the cross-section experiments.

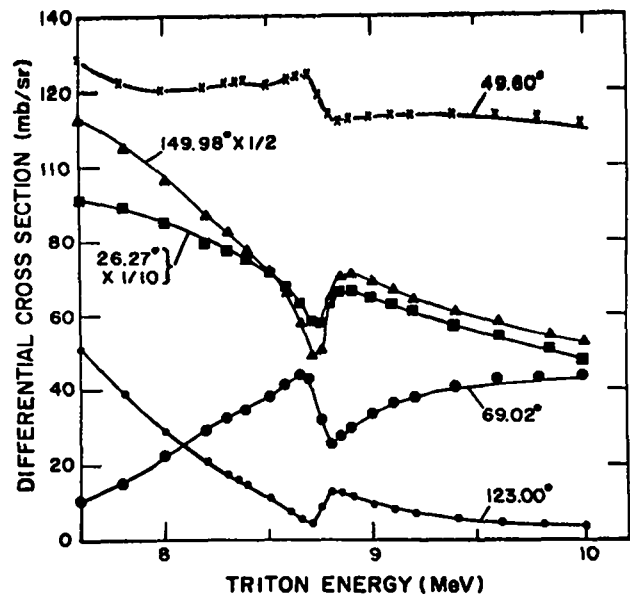


Fig. 8.  
Excitation functions for the  ${}^4\text{He}(t,t){}^4\text{He}$  differential cross section.

#### REFERENCES

1. R. A. Hardekopf, "Operation of the LASL Polarized Triton Source," Proc. 4th Int. Symp. Polariz. Phenom. Nucl. React., Zürich, 25-29 August 1975 (Birkhäuser Verlag, Basel, 1976), p. 865.
2. N. Jarmie, G. G. Ohlsen, P. A. Lovoi, D. M. Stupin, R. A. Hardekopf, B. D. Anderson, J. W. Sunier, R. V. Poore, R. J. Barrett, G. M. Hale, and D. C. Dodder, "Elastic Scattering of 7-12 MeV Tritons by Alpha Particles," to be published. Abstract in Bull. Am. Phys. Soc. 20, 596 (1975). See Phys. Rev. C3, 10 (1971) for experimental arrangement.
3. G. G. Ohlsen and P. A. Lovoi, "The 'Supercube' Scattering Chamber for Spin 1/2 and Spin 1 Analyzing Power Measurements," Proc. 4th Int. Symp. Polariz. Phenom. Nucl. React., Zürich, 25-29 August 1975 (Birkhäuser Verlag, Basel, 1976), p. 907.

4. P. A. Lovoi, "Proton-Proton Analyzing Power Measurements at 16 MeV," Ph.D. Dissertation, Univ. of New Mexico, 1975. Also Los Alamos Scientific Laboratory report LA-6041-T (September 1975).
5. G. G. Ohlsen, J. L. McKibben, G. P. Lawrence, P. W. Keaton, Jr., and D. D. Armstrong, "Precise Proton-Polarization Standards Determined with a Lamb-Shift Ion Source Incorporating a Nuclear Spin Filter," *Phys. Rev. Lett.* **27**, 599 (1971).
6. R. A. Hardekopf, G. G. Ohlsen, R. V. Poore, and N. Jarmie, "Calibration of a Polarized Triton Beam," *Proc. 4th Int. Symp. Polariz. Phenom. Nucl. React.*, Zürich, 25-29 August 1975 (Birkhäuser Verlag, Basel, 1976), p. 903.
7. G. G. Ohlsen and P. W. Keaton, Jr., "Techniques for Measurement of Spin-1/2 and Spin-1 Polarization Analyzing Tensors," *Nucl. Instrum. Methods* **109**, 42 (1973).
8. N. Jarmie, R. E. Brown, P. A. Schmelzbach, and R. F. Haglund, Jr., to be published.
9. Nelson Jarmie, J. H. Jett, and A. C. Niethammer, "SPANDY - A Monte Carlo Program for Simulation of Gas Target Scattering Geometry," Los Alamos Scientific Laboratory report LA-6611, to be published.
10. R. A. Hardekopf, G. G. Ohlsen, R. V. Poore, and N. Jarmie, "Location of a Polarization Extremum in Triton-Alpha Scattering and its Application to a New Polarized Triton Source," *Phys. Rev. C* **13**, 2127 (1976).
11. N. Jarmie and R. C. Allen, " $T(p,p)T$  Near the  $T(p,n)^4\text{He}$  Threshold," *Phys. Rev.* **114**, 176 (1959).
12. E. P. Wigner, "On the Behavior of Cross Sections Near Thresholds," *Phys. Rev.* **73**, 1002 (1948).
13. P. W. Keaton, Jr., D. D. Armstrong, and L. R. Veaser, "Polarization of Tritons Scattered from  $^4\text{He}$ ," *Phys. Rev. Lett.* **20**, 1392 (1968).
14. R. A. Hardekopf, N. Jarmie, G. G. Ohlsen, and R. V. Poore, "Analyzing Power for  $^4\text{He}(t,t)^4\text{He}$  Elastic Scattering," *Proc. 4th Int. Symp. Polariz. Phenom. Nucl. React.*, Zürich, 25-29 August 1975 (Birkhäuser Verlag, Basel, 1976), p. 579.
15. G. M. Hale, "R-Matrix Analysis of the Light Element Standards," in *Nuclear Cross-Sections and Technology*, Nat. Bur. Stand. Spec. Publ. 425, Vol. 1 (1975), p. 302.

## APPENDIX A

### ANALYZING POWER $A_y$ FOR ${}^4\text{He}(t,t){}^4\text{He}$

${}^4\text{He}(t,t){}^4\text{He}$ 8.785 MeV				${}^4\text{He}(t,t){}^4\text{He}$ 10.200 MeV			
$\theta_{\text{lab}}$ (deg)	$\theta_{\text{cm}}$ (deg)	$A_y(\theta)$	Error	$\theta_{\text{lab}}$ (deg)	$\theta_{\text{cm}}$ (deg)	$A_y(\theta)$	Error
15.0	26.3	-0.169	0.007	35.0	60.6	0.197	0.007
17.5	30.6	-0.157	0.007	37.5	64.8	-0.039	0.007
20.0	35.0	-0.132	0.007	40.0	69.0	-0.312	0.007
22.5	39.3	-0.103	0.007	42.5	73.2	-0.575	0.007
25.0	43.6	-0.055	0.007	45.0	77.2	-0.778	0.007
27.5	47.9	-0.003	0.007	47.5	81.3	-0.894	0.007
30.0	52.2	0.045	0.007	50.0	85.3	-0.963	0.007
32.5	56.4	0.090	0.007	45.0 <sup>a</sup>	90.0	-0.980	0.007
35.0	60.6	0.045	0.007	42.5 <sup>a</sup>	95.0	-0.986	0.007
37.5	64.8	-0.134	0.007	40.0 <sup>a</sup>	100.0	-0.951	0.007
40.0	69.0	-0.332	0.007	37.5 <sup>a</sup>	105.0	-0.919	0.007
42.5	73.2	-0.559	0.007	35.0 <sup>a</sup>	110.0	-0.884	0.007
45.0	77.2	-0.664	0.007				
47.5	81.3	-0.715	0.007				
50.0	85.3	-0.720	0.007				
52.5	89.3	-0.634	0.007				
55.0	93.2	-0.615	0.007				
57.5	97.0	-0.575	0.011				
40.0 <sup>a</sup>	100.0	-0.563	0.007				
37.5 <sup>a</sup>	105.0	-0.526	0.007				
35.0 <sup>a</sup>	110.0	-0.458	0.007				
32.5 <sup>a</sup>	115.0	-0.258	0.011				
30.0 <sup>a</sup>	120.0	0.168	0.010				
29.0 <sup>a</sup>	122.0	0.388	0.009				
27.5 <sup>a</sup>	125.0	0.627	0.008				
26.0 <sup>a</sup>	128.0	0.717	0.007				
25.0 <sup>a</sup>	130.0	0.710	0.007				
22.5 <sup>a</sup>	135.0	0.575	0.007				
20.0 <sup>a</sup>	140.0	0.446	0.007				
17.5 <sup>a</sup>	145.0	0.350	0.007				
15.0 <sup>a</sup>	150.0	0.257	0.007				

<sup>a</sup> alpha particle detected.

<sup>a</sup> alpha particle detected.

${}^4\text{He}(t,t){}^4\text{He}$  10.815 MeV

$\theta_{\text{lab}}$ (deg)	$\theta_{\text{cm}}$ (deg)	$A_Y(\theta)$	Error	$\theta_{\text{lab}}$ (deg)	$\theta_{\text{cm}}$ (deg)	$A_Y(\theta)$	Error
16.0	28.0	0.216	0.007	44.0 <sup>a</sup>	92.0	-1.006	0.007
18.0	31.5	0.279	0.007	56.0	94.7	-1.004	0.007
20.0	35.0	0.340	0.007	42.5 <sup>a</sup>	95.0	-1.002	0.007
22.0	38.4	0.400	0.007	42.0 <sup>a</sup>	96.0	-0.997	0.007
24.0	41.9	0.444	0.007	58.0	97.8	-1.002	0.008
26.0	45.3	0.478	0.007	40.0 <sup>a</sup>	100.0	-0.979	0.010
28.0	48.8	0.490	0.007	38.0 <sup>a</sup>	104.0	-0.958	0.012
30.0	52.2	0.477	0.007	37.5 <sup>a</sup>	105.0	-0.968	0.007
32.0	55.6	0.421	0.007	37.0 <sup>a</sup>	106.0	-0.980	0.007
34.0	59.0	0.309	0.007	36.0 <sup>a</sup>	108.0	-0.971	0.010
35.0	60.6	0.237	0.007	35.0 <sup>a</sup>	110.0	-0.965	0.007
36.0	62.3	0.143	0.007	34.0 <sup>a</sup>	112.0	-0.907	0.012
37.0	64.0	0.052	0.007	33.0 <sup>a</sup>	114.0	-0.855	0.013
37.5	64.8	0.003	0.007	32.0 <sup>a</sup>	116.0	-0.566	0.018
38.0	65.7	-0.045	0.008	31.0 <sup>a</sup>	118.0	-0.090	0.023
40.0	69.0	-0.267	0.007	30.5 <sup>a</sup>	119.0	0.158	0.020
42.0	72.3	-0.480	0.009	30.0 <sup>a</sup>	120.0	0.375	0.020
42.5	73.2	-0.531	0.007	29.5 <sup>a</sup>	121.0	0.420	0.018
44.0	75.6	-0.664	0.008	29.0 <sup>a</sup>	122.0	0.430	0.016
45.0	77.2	-0.732	0.007	28.5 <sup>a</sup>	123.0	0.369	0.015
46.0	78.9	-0.799	0.008	28.0 <sup>a</sup>	124.0	0.302	0.013
47.5	81.3	-0.869	0.007	27.0 <sup>a</sup>	126.0	0.150	0.013
48.0	82.1	-0.918	0.007	26.0 <sup>a</sup>	128.0	0.056	0.012
48.0 <sup>a</sup>	84.0	-0.939	0.007	25.5 <sup>a</sup>	129.0	0.004	0.009
50.0	85.3	-0.946	0.007	24.0 <sup>a</sup>	132.0	-0.089	0.008
46.0 <sup>a</sup>	88.0	-0.981	0.007	22.0 <sup>a</sup>	136.0	-0.174	0.008
52.0	88.5	-0.984	0.007	20.0 <sup>a</sup>	140.0	-0.204	0.010
45.0 <sup>a</sup>	90.0	-0.999	0.007	18.0 <sup>a</sup>	144.0	-0.232	0.010
54.0	91.6	-0.990	0.007	16.0 <sup>a</sup>	148.0	-0.266	0.010

<sup>a</sup> alpha particle detected.

${}^4\text{He}(t,t){}^4\text{He}$  11.100 MeV

$\theta_{\text{lab}}$ (deg)	$\theta_{\text{cm.}}$ (deg)	$A_Y(\theta)$	Error
32.5	56.4	0.432	0.007
35.0	60.6	0.270	0.007
37.5	64.8	0.030	0.007
40.0	69.0	-0.266	0.007
42.5	73.2	-0.526	0.007
45.0	77.2	-0.737	0.007
47.5	81.3	-0.881	0.007
50.0	85.3	-0.948	0.007
45.0 <sup>a</sup>	90.0	-1.000	0.007
42.5 <sup>a</sup>	95.0	-1.006	0.007
40.0 <sup>a</sup>	100.0	-1.000	0.007
37.5 <sup>a</sup>	105.0	-0.995	0.007
35.0 <sup>a</sup>	110.0	-0.975	0.007
32.5 <sup>a</sup>	115.0	-0.720	0.013

<sup>a</sup> alpha particle detected. ${}^4\text{He}(t,t){}^4\text{He}$  11.700 MeV

$\theta_{\text{lab}}$ (deg)	$\theta_{\text{cm.}}$ (deg)	$A_Y(\theta)$	Error
35.0	60.6	0.348	0.007
37.5	64.8	0.069	0.007
40.0	69.0	-0.269	0.007
42.5	73.2	-0.579	0.007
45.0	77.2	-0.795	0.007
47.5	81.3	-0.902	0.007
47.5 <sup>a</sup>	85.0	-0.960	0.007
45.0 <sup>a</sup>	90.0	-0.986	0.007
42.5 <sup>a</sup>	95.0	-0.988	0.007
40.0 <sup>a</sup>	100.0	-0.981	0.007
37.5 <sup>a</sup>	105.0	-0.973	0.007
35.0 <sup>a</sup>	110.0	-0.920	0.007

<sup>a</sup> alpha particle detected. ${}^4\text{He}(t,t){}^4\text{He}$  11.390 MeV

$\theta_{\text{lab}}$ (deg)	$\theta_{\text{cm.}}$ (deg)	$A_Y(\theta)$	Error
35.0	60.6	0.320	0.007
37.5	64.8	0.051	0.007
40.0	69.0	-0.246	0.007
42.5	73.2	-0.537	0.007
45.0	77.2	-0.750	0.007
47.5	81.3	-0.890	0.007
50.0	85.3	-0.957	0.007
45.0 <sup>a</sup>	90.0	-0.988	0.007
42.5 <sup>a</sup>	95.0	-0.998	0.007
40.0 <sup>a</sup>	100.0	-0.992	0.007
37.5 <sup>a</sup>	105.0	-1.002	0.007
35.0 <sup>a</sup>	110.0	-0.962	0.008

<sup>a</sup> alpha particle detected. ${}^4\text{He}(t,t){}^4\text{He}$  12.250 MeV

$\theta_{\text{lab}}$ (deg)	$\theta_{\text{cm.}}$ (deg)	$A_Y(\theta)$	Error
15.0	26.3	0.727	0.007
17.5	30.6	0.801	0.007
20.0	35.0	0.851	0.007
22.5	39.3	0.886	0.007
25.0	43.6	0.909	0.007
27.5	47.9	0.896	0.007
30.0	52.2	0.867	0.007
32.5	56.4	0.795	0.007
35.0	60.6	0.578	0.007
37.5	64.8	0.124	0.007
40.0	69.0	-0.505	0.008
42.5	73.2	-0.851	0.007
45.0	77.2	-0.933	0.007
47.5	81.3	-0.895	0.007
47.5 <sup>a</sup>	85.0	-0.873	0.007
45.0 <sup>a</sup>	90.0	-0.819	0.009
42.5 <sup>a</sup>	95.0	-0.810	0.008
40.0 <sup>a</sup>	100.0	-0.806	0.007
37.5 <sup>a</sup>	105.0	-0.772	0.009
35.0 <sup>a</sup>	110.0	-0.580	0.009
32.5 <sup>a</sup>	115.0	-0.117	0.009
31.25 <sup>a</sup>	117.5	0.202	0.010
30.0 <sup>a</sup>	120.0	0.512	0.009
28.75 <sup>a</sup>	122.5	0.591	0.009
27.5 <sup>a</sup>	125.0	0.467	0.008
26.25 <sup>a</sup>	127.5	0.197	0.008
25.0 <sup>a</sup>	130.0	-0.062	0.008
22.5 <sup>a</sup>	135.0	-0.481	0.007
20.0 <sup>a</sup>	140.0	-0.746	0.007
17.5 <sup>a</sup>	145.0	-0.889	0.007
15.0 <sup>a</sup>	150.0	-0.950	0.007

<sup>a</sup> alpha particle detected.

${}^4\text{He}(t,t){}^4\text{He}$   
Excitation Function  $\theta_{\text{lab}} = 28.5 \text{ deg}$

Et (MeV)	tritons		alphas		Et (MeV)	tritons		alphas	
	$\theta_{\text{cm}} = 49.6 \text{ deg}$ $A_Y(\theta)$	Error	$\theta_{\text{cm}} = 123.0 \text{ deg}$ $A_Y(\theta)$	Error		$\theta_{\text{cm}} = 49.6 \text{ deg}$ $A_Y(\theta)$	Error	$\theta_{\text{cm}} = 123.0 \text{ deg}$ $A_Y(\theta)$	Error
7.000	-0.804	0.007			9.600	0.377	0.007	0.269	0.014
7.100	-0.802	0.007			9.800	0.395	0.007	0.272	0.017
7.200	-0.767	0.007			10.000	0.413	0.007		
7.300	-0.706	0.007			10.200	0.427	0.007		
7.400	-0.616	0.007			10.400	0.440	0.007		
7.500	-0.501	0.007			10.600	0.463	0.007		
7.600	-0.374	0.007			10.800	0.485	0.007		
7.800	-0.108	0.007	0.273	0.008	11.000	0.515	0.007		
8.000	0.073	0.007	0.279	0.008	11.200	0.548	0.007		
8.200	0.202	0.007	0.253	0.008	11.400	0.585	0.007		
8.300	0.242	0.007	0.253	0.008	11.600	0.633	0.007		
8.350	0.261	0.007			11.800	0.681	0.007		
8.375	0.271	0.007			12.000	0.748	0.007		
8.400	0.268	0.007	0.214	0.008	12.200	0.848	0.007		
8.425	0.279	0.007			12.300	0.910	0.007		
8.450	0.288	0.007			12.400	0.952	0.007		
8.475	0.294	0.007			12.500	0.933	0.007		
8.500	0.304	0.007	0.191	0.010	12.600	0.804	0.007		
8.550	0.310	0.007			12.700	0.642	0.007		
8.600	0.299	0.007	0.254	0.013	12.800	0.503	0.007		
8.650	0.277	0.007	0.492	0.011	12.900	0.416	0.007		
8.700	0.126	0.007	0.770	0.011	13.000	0.356	0.007		
8.750	-0.023	0.007	0.596	0.011	13.200	0.316	0.007		
8.800	0.024	0.007	0.431	0.011	13.400	0.299	0.007		
8.850	0.131	0.007			13.500	0.306	0.007		
8.900	0.208	0.007	0.358	0.012	13.600	0.304	0.007		
9.000	0.278	0.007			13.700	0.294	0.007		
9.100	0.314	0.007			13.800	0.307	0.007		
9.200	0.338	0.007			14.000	0.289	0.007		
9.400	0.365	0.007	0.257	0.013	14.200	0.293	0.007		

${}^4\text{He}(t,t){}^4\text{He}$   
Excitation Function  $\theta_{\text{lab}} = 35.0 \text{ deg}$

Et (MeV)	tritons		alphas	
	$\theta_{\text{cm}} = 60.6 \text{ deg}$ $A_Y(\theta)$	Error	$\theta_{\text{cm}} = 110.0 \text{ deg}$ $A_Y(\theta)$	Error
8.200	0.212	0.008	-0.398	0.010
8.300	0.202	0.008	-0.420	0.010
8.350	0.191	0.007	-0.435	0.010
8.375	0.190	0.007	-0.447	0.010
8.400	0.182	0.007	-0.457	0.010
8.425	0.178	0.007	-0.476	0.010
8.450	0.182	0.007	-0.482	0.010
8.475	0.181	0.007	-0.500	0.010
8.500	0.185	0.007	-0.502	0.010
8.550	0.161	0.007	-0.548	0.010
8.600	0.145	0.007	-0.608	0.010
8.700	0.063	0.007	-0.642	0.010

## APPENDIX B

### DIFFERENTIAL CROSS SECTIONS $\sigma(\theta)$ FOR ${}^4\text{He}(t,t){}^4\text{He}$

${}^4\text{He}(t,t){}^4\text{He}$  8.230 MeV  
Scale Error = 0.40%

${}^4\text{He}(t,t){}^4\text{He}$  8.580 MeV  
Scale Error = 0.40%

$\theta_{\text{lab}}$ (deg)	$(\theta)_{\text{lab}}$ (mb/sr)	$\theta_{\text{c.m.}}$ (deg)	$\sigma(\theta)_{\text{c.m.}}$ (mb/sr)	Rel. Error (%)	$\theta_{\text{lab}}$ (deg)	$\sigma(\theta)_{\text{lab}}$ (mb/sr)	$\theta_{\text{c.m.}}$ (deg)	$\sigma(\theta)_{\text{c.m.}}$ (mb/sr)	Rel. Error (%)
12.50	3247.0	21.90	1078.0	0.60	12.50	2812.0	21.90	933.9	0.40
15.00	2364.0	26.27	793.1	0.40	15.00	2025.0	26.27	679.3	0.40
20.00	1275.0	34.96	439.1	0.40	20.00	1102.0	34.96	379.3	0.40
22.50	900.5	39.29	314.9	0.40	25.00	562.3	43.60	200.2	0.40
25.00	613.7	43.60	218.5	0.40	30.00	268.9	52.17	99.81	0.40
27.50	400.7	47.89	145.5	0.40	35.00	138.5	60.65	54.07	0.49
30.00	251.0	52.17	93.21	0.45	40.00	98.71	69.01	40.93	0.49
32.50	156.1	56.42	59.34	0.50	45.00	95.01	77.24	42.26	0.52
35.00	100.60	60.65	39.27	0.60	50.00	91.59	85.30	44.18	0.46
37.50	77.04	64.84	30.96	0.60	55.00	78.65	93.16	41.60	0.71
40.00	72.79	69.01	30.19	0.60	35.00 <sup>a</sup>	63.27	109.96	19.30	0.9
45.00	92.80	77.24	41.28	0.50	32.50 <sup>a</sup>	40.25	115.00	11.93	0.9
50.00	111.1	85.30	53.61	0.70	30.00 <sup>a</sup>	27.87	119.97	8.041	1.0
35.00 <sup>a</sup>	115.7	109.97	35.31	2.0	27.50 <sup>a</sup>	32.59	124.97	9.181	1.1
32.50 <sup>a</sup>	87.84	114.97	26.03	0.9	25.00 <sup>a</sup>	61.51	129.97	16.96	1.5
30.00 <sup>a</sup>	68.98	119.97	19.90	0.9	20.00 <sup>a</sup>	219.6	139.98	58.37	0.70
27.50 <sup>a</sup>	71.68	124.97	20.19	1.0	15.00 <sup>a</sup>	504.1	149.97	130.3	0.60
25.00 <sup>a</sup>	106.1	129.98	29.26	1.1	12.50 <sup>a</sup>	670.7	155.01	171.6	0.60
22.50 <sup>a</sup>	180.5	134.98	48.81	0.90					
20.00 <sup>a</sup>	301.3	139.98	80.09	0.80					
15.00 <sup>a</sup>	653.7	149.98	169.0	0.60					
12.50 <sup>a</sup>	871.7	154.99	223.0	0.60					

<sup>a</sup>Alpha particle detected.

<sup>a</sup>Alpha particle detected.

${}^4\text{He}(t,t){}^4\text{He}$  8.790 MeV  
Scale Error = 0.40%

${}^4\text{He}(t,t){}^4\text{He}$  3.980 MeV  
Scale Error = 0.40%

$\theta_{\text{lab}}$ (deg)	$\sigma(\theta)_{\text{lab}}$ (mb/sr)	$\theta_{\text{c.m.}}$ (deg)	$\sigma(\theta)_{\text{c.m.}}$ (mb/sr)	Rel. Error (%)	$\theta_{\text{lab}}$ (deg)	$\sigma(\theta)_{\text{lab}}$ (mb/sr)	$\theta_{\text{c.m.}}$ (deg)	$\sigma(\theta)_{\text{c.m.}}$ (mb/sr)	Rel. Error (%)
12.50	2549.0	21.90	846.5	0.46	12.50	2636.0	21.90	875.4	0.40
25.00	539.1	43.59	191.9	0.40	15.00	1932.0	26.27	648.1	0.40
30.00	240.8	52.17	89.37	0.40	20.00	1062.0	34.96	365.7	0.40
37.57	72.25	64.97	29.06	0.60	22.50	760.5	39.29	265.9	0.40
40.00	62.28	69.00	25.83	0.60	25.00	534.7	43.60	190.3	0.40
45.00	66.26	77.25	29.47	0.56	27.50	364.9	47.88	132.5	0.40
50.00	76.43	85.29	36.86	0.70	30.00	243.4	52.16	90.34	0.40
55.00	74.50	93.17	39.40	0.90	32.50	165.9	56.43	63.09	0.40
37.50 <sup>a</sup>	88.85	104.96	27.99	1.0	35.00	113.5	60.64	44.33	0.50
35.00 <sup>a</sup>	70.10	109.97	21.38	1.0	37.50	89.14	64.86	35.83	0.58
32.50 <sup>a</sup>	51.82	114.97	15.36	1.1	40.00	79.91	69.01	33.13	0.62
30.00 <sup>a</sup>	41.10	119.97	11.85	1.3	45.00	83.64	77.24	37.20	0.51
25.00 <sup>a</sup>	76.25	129.97	21.02	1.3	50.00	88.09	85.30	42.50	0.51
20.00 <sup>a</sup>	225.5	139.99	59.94	1.0	55.00	79.96	93.16	42.34	0.70
16.76 <sup>a</sup>	388.0	146.50	101.2	0.90	37.50 <sup>a</sup>	89.40	104.96	28.16	1.1
15.00 <sup>a</sup>	485.0	149.99	125.4	0.80	35.00 <sup>a</sup>	67.68	109.98	20.64	0.9
12.50 <sup>a</sup>	638.1	154.99	163.2	0.70	32.50 <sup>a</sup>	46.06	114.96	13.65	1.0
					30.00 <sup>a</sup>	33.96	119.98	9.796	1.0
					27.50 <sup>a</sup>	39.36	124.97	11.09	1.6
					25.00 <sup>a</sup>	71.44	129.97	19.69	1.2
					22.50 <sup>a</sup>	138.4	134.98	37.41	1.0
					20.00 <sup>a</sup>	240.6	139.98	63.93	0.80
					15.00 <sup>a</sup>	534.0	149.98	138.1	0.70
					12.50 <sup>a</sup>	711.9	154.99	182.1	0.60

<sup>a</sup>Alpha particle detected.

<sup>a</sup>Alpha particle detected.



${}^4\text{He}(t,t){}^4\text{He}$  9.880 MeV  
Scale Error = 0.40%

${}^4\text{He}(t,t){}^4\text{He}$  12.00 MeV  
Scale Error = 0.40%

$\theta_{\text{lab}}$ (deg)	$\sigma(\theta)_{\text{lab}}$ (mb/sr)	$\theta_{\text{c.m.}}$ (deg)	$\sigma(\theta)_{\text{c.m.}}$ (mb/sr)	Rel. Error (%)	$\theta_{\text{lab}}$ (deg)	$\sigma(\theta)_{\text{lab}}$ (mb/sr)	$\theta_{\text{c.m.}}$ (deg)	$\sigma(\theta)_{\text{c.m.}}$ (mb/sr)	Rel. Error (%)
12.50	2023.0	21.91	671.6	0.40	12.50	1187.0	21.91	393.9	0.40
15.00	1494.0	26.27	501.2	0.42	15.00	988.6	26.27	331.5	0.40
20.00	856.2	34.96	294.7	0.40	20.00	685.7	34.97	235.9	0.40
25.00	476.00	43.60	169.4	0.40	25.00	432.7	43.61	154.0	0.40
30.00	255.6	52.17	94.88	0.40	30.00	236.7	52.18	87.85	0.40
30.00	257.1	52.17	95.44	0.40	35.00	117.7	60.66	45.93	0.50
32.50	190.3	56.41	72.38	0.40	40.00	71.78	69.02	29.76	0.60
35.00	146.6	60.65	57.23	0.42	45.00	67.50	77.26	30.02	0.56
36.63	128.4	63.39	51.08	0.37	50.00	71.61	85.31	34.54	0.51
37.50	120.2	64.83	48.29	0.47	45.00 <sup>a</sup>	98.84	89.95	34.95	0.70
40.00	104.8	69.02	43.45	0.52	40.00 <sup>a</sup>	78.79	99.97	25.70	0.80
42.50	94.59	73.14	40.56	0.45	35.00 <sup>a</sup>	34.95	109.96	10.66	1.2
45.00	88.30	77.25	39.20	0.40	30.00 <sup>a</sup>	15.92	119.96	4.591	2.0
47.50	81.80	81.30	37.83	0.51	25.00 <sup>a</sup>	71.04	129.97	19.60	1.2
50.00	76.32	85.29	36.70	0.45	20.00 <sup>a</sup>	195.6	139.97	51.99	1.0
52.50	68.59	89.27	34.61	0.51	15.00 <sup>a</sup>	339.2	149.98	87.69	0.70
53.85	63.62	91.38	32.94	0.90	12.50 <sup>a</sup>	403.8	154.90	103.3	0.70
55.00	58.36	93.17	30.90	2.00					
57.50	48.82	97.00	27.21	0.80					
40.00 <sup>a</sup>	73.11	99.96	23.85	0.61					
35.05 <sup>a</sup>	33.88	109.89	10.335	0.84					
30.00 <sup>a</sup>	9.924	119.97	2.863	1.2					
25.00 <sup>a</sup>	50.96	129.99	14.05	0.80					
20.00 <sup>a</sup>	188.0	139.98	49.96	0.80					
15.00 <sup>a</sup>	398.1	150.00	102.9	0.49					
15.00 <sup>a</sup>	398.3	150.00	103.0	0.50					
12.50 <sup>a</sup>	507.5	154.92	129.8	0.90					

<sup>a</sup>Alpha particle detected.

<sup>a</sup>Alpha particle detected.

${}^4\text{He}(t,t){}^4\text{He}$  (15.00° lab) Tritons Detected  
Scale Error = 0.40%

$E_t$ (MeV)	$\sigma(\theta)$ lab (mb/sr)	$\theta$ c.m. (deg)	$\sigma(\theta)$ c.m. (mb/sr)	Rel. error (%)
7.600	2728.0	26.26	915.3	0.40
7.800	2657.0	26.25	891.4	0.40
8.000	2529.0	26.26	848.4	0.40
8.200	2387.0	26.27	801.0	0.40
8.300	2311.0	26.27	775.5	0.40
8.391	2240.0	26.27	751.3	0.40
8.500	2136.0	26.26	716.7	0.40
8.580	2031.0	26.26	681.4	0.40
8.650	1888.0	26.27	633.3	0.40
8.700	1745.0	26.27	585.6	0.40
8.750	1720.0	26.27	576.9	0.40
8.800	1881.0	26.27	630.9	0.40
8.850	1971.0	26.27	661.2	0.40
8.900	1979.0	26.27	663.9	0.40
9.000	1924.0	26.27	645.5	0.40
9.100	1859.0	26.27	623.4	0.40
9.200	1809.0	26.27	606.9	0.40
9.400	1704.0	26.28	571.7	0.40
9.600	1608.0	26.28	539.2	0.40
9.844	1517.0	26.28	508.9	0.40
10.000	1446.0	26.27	484.8	0.40

${}^4\text{He}(t,t){}^4\text{He}$  (28.50° lab) Tritons Detected:  
Excitation Function  
Scale Error = 0.40%

$E_t$ (MeV)	$\sigma(\theta)$ lab (mb/sr)	$\theta$ c.m. (deg)	$\sigma(\theta)$ c.m. (mb/sr)	Rel. error (%)
7.600	354.3	49.58	129.8	0.40
7.800	336.6	49.58	123.3	0.40
8.000	332.7	49.59	121.9	0.40
8.200	334.2	49.59	122.4	0.40
8.300	336.8	49.59	123.4	0.40
8.350	337.4	49.59	123.6	0.40
8.391	338.4	49.58	123.9	0.40
8.500	334.9	49.60	122.6	0.40
8.600	339.0	49.60	124.2	0.40
8.650	340.6	49.60	124.8	0.40
8.700	342.0	49.61	125.3	0.40
8.750	328.4	49.60	120.3	0.40
8.800	313.8	49.61	114.9	0.40
8.850	307.7	49.61	112.7	0.40
8.900	309.9	49.61	113.5	0.40
9.000	311.9	49.62	114.2	0.40
9.100	312.7	49.61	114.5	0.40
9.200	312.9	49.61	114.6	0.40
9.400	313.7	49.60	114.9	0.40
9.600	312.5	49.60	114.4	0.40
9.800	309.9	49.60	113.5	0.40
10.000	306.1	49.60	112.1	0.40

${}^4\text{He}(t,t){}^4\text{He}$  (40.00° lab) Tritons Detected  
Scale Error = 0.40%

${}^4\text{He}(t,t){}^4\text{He}$  (28.50° lab) Alphas Detected  
Scale Error = 0.40%

$E_t$ (MeV)	$\sigma(\theta)_{\text{lab}}$ (mb/sr)	$\theta_{\text{c.m.}}$ (deg)	$\sigma(\theta)_{\text{c.m.}}$ (mb/sr)	Rel. Error (%)	$E_t$ (MeV)	$\sigma(\theta)_{\text{lab}}$ (mb/sr)	$\theta_{\text{c.m.}}$ (deg)	$\sigma(\theta)_{\text{c.m.}}$ (mb/sr)	Rel. Error (%)
7.600	26.92	69.00	11.16	0.90	7.600	174.2	123.01	49.52	3.0
7.800	37.09	69.01	15.38	0.90	7.800	133.0	123.01	37.80	3.0
8.000	53.86	69.01	22.34	0.80	8.000	98.65	122.99	28.04	3.0
8.200	69.97	69.00	29.01	0.75	8.200	70.97	122.99	20.18	3.0
8.300	77.95	69.01	32.32	0.75	8.300	59.76	122.99	16.98	3.0
8.391	82.71	69.01	34.29	0.75	8.350	54.65	122.99	15.54	3.0
8.500	90.92	69.01	37.70	0.70	8.391	49.85	123.0	14.17	3.0
8.580	99.61	69.01	41.31	0.70	8.500	38.05	122.97	10.82	3.0
8.650	105.9	69.01	43.93	0.70	8.600	25.31	122.97	7.194	3.0
8.700	103.2	69.01	42.78	0.70	8.650	18.33	122.97	5.211	3.0
8.750	76.02	69.01	31.52	0.75	8.700	15.10	122.97	4.292	3.0
8.800	61.39	69.01	25.46	0.75	8.750	29.62	122.98	8.422	3.0
8.850	66.97	69.01	27.77	0.70	8.800	42.56	122.97	12.10	3.0
8.900	71.44	69.01	29.62	0.70	8.850	42.39	122.97	12.05	4.0
9.000	81.24	69.02	33.68	0.65	8.900	39.05	122.97	11.10	4.0
9.100	87.82	69.02	36.42	0.65	9.000	31.63	122.96	8.994	4.0
9.200	91.55	69.02	37.95	0.65	9.100	27.17	122.97	7.724	4.0
9.400	98.13	69.02	40.69	0.65	9.200	23.74	122.97	6.748	5.0
9.600	102.0	69.02	42.28	0.60	9.400	19.20	122.98	5.460	5.0
9.800	103.0	69.02	42.70	0.60	9.600	16.16	122.98	4.592	6.0
10.000	105.6	69.02	43.76	0.60	9.800	13.89	122.98	3.947	6.0
					10.000	12.76	122.99	3.628	6.0

${}^4\text{He}(t,t){}^4\text{He}$  (15.00° lab) Alphas Detected  
 Scale Error = 0.40%

$E_t$ (MeV)	$\sigma(\theta)_{\text{lab}}$ (mb/sr)	$\theta_{\text{c.m.}}$ (deg)	$\sigma(\theta)_{\text{c.m.}}$ (mb/sr)	Rel. error (%)
7.600	889.9	149.99	230.1	0.53
7.800	829.0	150.00	214.4	0.54
8.000	754.7	149.99	195.1	0.57
8.200	677.0	149.97	175.1	0.59
8.300	640.8	149.98	165.7	0.60
8.391	597.2	149.98	154.4	0.62
8.500	556.9	149.99	144.0	0.65
8.580	504.2	149.98	130.4	0.58
8.650	434.7	149.97	112.4	0.62
8.700	362.2	149.97	93.64	0.67
8.750	373.2	149.98	96.48	0.77
8.800	494.0	149.97	127.7	0.67
8.850	540.7	149.97	139.8	0.64
8.900	546.7	149.97	141.3	0.64
9.000	528.6	149.97	136.7	0.65
9.100	509.2	149.97	131.7	0.66
9.200	488.9	149.98	126.4	0.67
9.400	459.0	149.97	118.7	0.69
9.600	437.3	149.97	113.1	0.70
9.844	409.2	149.97	105.8	0.72
10.000	393.9	149.98	101.8	0.74